Supplementary material to: On asymmetric vortex pair interactions in shear

Patrick J. R. Folz[1]†, Keiko K. Nomura[1]

[1]Department of Mechanical and Aerospace Engineering, University of California, San Diego, 9500 Gilman Drive, La Jolla, CA, 92093-0411, USA

In this supplementary material, the time evolution of the key quantities utilized in the flow analysis — namely, core area, A_{II}, core circulation, Γ_{II}, and relative straining, $(S/\omega)_i$ — are presented for example cases of a single vortex in shear (§S1) and vortex pairs in shear (§S2), accompanied by brief description highlighting salient features. This reference is intended to benefit readers desiring a fuller understanding the flow development and the quantities utilized to compute the outcome quantities ε and η.

As indicated in the main text, the core area and circulation correspond to the aggregate flow region meeting the threshold, $II > II_t$, where $II = 1/2(\omega^2/2 - S^2)$ is the second invariant at a given location and time, and the threshold $II_t^* = II/II_{peak} = 0.10$:

$$A_{II} = \int_{II>II_t} dA$$

and

$$\Gamma_{II} = \int_{II>II_t} \omega dA,$$

where dA refers to an area element of fluid. See main text and Folz & Nomura (2017) for details.

These simulations are all performed using the computational methods described in §3 of the main text. Note that these simulations were terminated after the main convective interaction has been completed and the final vortex has begun to axisymmetrize, in order to conserve computational resources; the end times of each curve therefore have no significant physical meaning.

S1. Single vortex in shear

This section briefly reviews the flow development of a single vortex in favorable and adverse shear, a useful reference when considering the pair case. In the adverse case, the start of core detrainment is identified and found to correspond to a critical $(S/\omega)_{cr}$ value similar to that found for pairs in Folz & Nomura (2017).

A single vortex in shear deforms elliptically along a direction roughly orthogonal to or aligned with the shear direction in favourable or adverse shear, respectively, and in the adverse case, the intensifying deformation and relative straining eventually leads to filamentation — i.e. detrainment — and breakup, as discussed in §1 and references therein. These processes are reflected in the time evolution of A_{II}, Γ_{II}, and (S/ω), which are presented in figure S1 along with the instantaneous shear strength $|\zeta|$, for a single vortex in favourable and adverse shear, respectively, having $|\zeta_0 = 0.01|$ and $Re_\Gamma = 1000$ (in order to accelerate the flow development

† Email address for correspondence: pjfolz@ucsd.edu

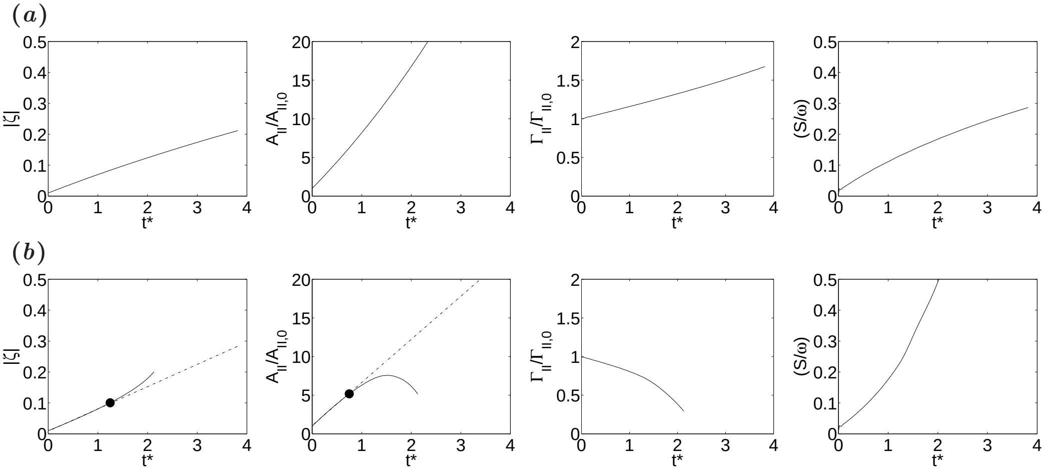

Figure S1: Time development of shear strength parameter magnitude $|\zeta|$, and key quantities: normalized core area $A_{II}/A_{II,0}$, normalized core circulation $\Gamma_{II}/\Gamma_{II,0}$, and relative straining S/ω, for a single vortex: (a) favourable shear ($\zeta_0 = 0.01$), and (b) adverse shear ($\zeta_0 = -0.01$). In (b), the dash-dot line indicates the linear fit to the early portion used to ascertain the time of departure from linear behavior (• at $t^* = 1.25$ in ζ plot, and $t^* = 0.75$ in $A_{II}/A_{II,0}$ plot). This departure is found by computing the correlation coefficient (R^2) for a linear fit to progressively larger portions of the time development (beginning with the first $N = 20$ output times) until R^2 falls below a pre-selected threshold value ($R^2_{thresh} = 0.999$).

for better visualization of the major processes). In all cases, $|\zeta(t)| = \alpha/\omega(t)$ increases continuously due to viscous diffusion reducing ω. For reference, in the case of a single vortex diffusing without shear ($\zeta_0 = 0$), A_{II} grows linearly and Γ_{II} remains constant (shown in Folz & Nomura 2017), while the relative straining of this vortex remains $(S/\omega) = 0$ (consistent with no deformation).

It is seen that, in favourable shear ($\zeta_0 > 0$), ζ, A_{II}, Γ_{II}, and S/ω all increase monotonically throughout the flow development, which consists of viscous spreading, elliptical deformation, and little else (the increase of Γ_{II} here, where it was constant in the no-shear case, results from the use of II_t as the vortex diffuses and deforms). The increasing deformation results from the intensifying shear strength ζ and is reflected in the increasing of S/ω. Although there is a slight growth acceleration of A_{II} and Γ_{II}, and deceleration of S/ω and ζ over the entire flow development, the growth of each of these quantities could reasonably be approximated as linear in this case (a linear fit with $R^2 = 0.99$ can be made to each, not shown). These processes continue until the ultimate dissipation of the vortex.

Conversely, in adverse shear ($\zeta_0 < 0$), a significant qualitative change in the behavior of key quantities is observed, reflecting detrainment of the core and subsequent breakup. The shear strength magnitude $|\zeta|$ again increases monotonically, but this growth is seen to accelerate significantly in the latter portion of the flow development (at $t^* \approx 1.25$, see figure S1 caption). The growth of A_{II}, after an initial approximately linear increase, begins to decelerate (earlier than $|\zeta|$'s acceleration), reaching a local maximum and then decreasing; Γ_{II} declines approximately linearly at first, then more rapidly beginning at approximately the same time as A_{II}'s deviation from linear (at $t^* \approx 0.75$). The growth of S/ω

is likewise monotonic and accelerates slightly throughout, but most significantly when $|\zeta|$ does as well. The deviation of A_{II} growth from linear coincides with the start of *core* detrainment (note that filamentation of low-level, i.e. non-core, peripheral vorticity occurs before this time); this detrainment is reflected in the accelerating decline of Γ_{II}. In other words, the deviation of A_{II} from linear growth in this case reflects the transition from viscosity-dominated to convection-dominated flow development, as it did in the case of no-shear pairs (see e.g. Brandt & Nomura 2007; recall also that adverse shear approximates the influence of a co-rotating vortex pair partner, see §1). The later deviation of $|\zeta|$'s growth from linear (as well as the concomitant significant acceleration of S/ω's) reflects the final, rapid *breakup* of the vortex, during which the $II > II_t$ core is swiftly eroded away and the vortex is ultimately dissipated (see e.g. Mariotti *et al.* 1994).

Significantly, the deviation of A_{II} from linear growth — the start of core detrainment — and the transition from viscosity-dominated to convection-dominated flow development occurs when $S/\omega \approx 0.128$, very close to the critical value of $(S/\omega)_{cr} \approx 0.135 \pm 0.03$ associated with detrainment in no-shear pairs (Folz & Nomura 2017; the estimate made here derives in part from additional simulations having $\zeta_0 = -0.005$ and $\zeta_0 = -0.02$, not shown). This suggests that this critical value associated with core detrainment is generally consistent for a Gaussian vortex in viscous flow. The value of ζ associated with vortex *breakup*, $\zeta_{bu} \approx -0.10$, is comparable to the values $\zeta_{bu} = -0.10$ to -0.13 found by Mariotti *et al.* (1994) and Paireau *et al.* (1997).

These observations and critical values inform the discussion and analysis of vortex pairs in shear.

S2. Vortex pairs in shear

This section briefly reviews the flow development of vortex pairs, which may be unequal, in both favorable and adverse shear, utilizing the core quantities A_{II} and Γ_{II}, as well as the relative straining of both the weaker and stronger vortices, $(S/\omega)_1$ and $(S/\omega)_2$, respectively.

First, the time development of these quantities in no-shear flow, observed in Folz & Nomura (2017), is here briefly reviewed: A_{II} grows approximately linearly during the viscosity-dominated portion of the interaction, then declines and, in some cases, thereafter spikes during the convection-dominated portion, corresponding to detrainment and entrainment, respectively; Γ_{II} declines slightly but steadily during the viscosity-dominated portion (due to the vortices' intensifying mutual strain), followed by a more rapid drop during detrainment, and then a spike in cases in which entrainment occurs; and $(S/\omega)_i$ grows continuously throughout both the viscosity-dominated and convection-dominated portions, through the end of detrainment (at which point either the vortex is destroyed, or, if it is the "winner" of the interaction, $(S/\omega)_i$ then declines during reaxisymmetrization). Significantly, the initiation of detrainment of a vortex is seen to be associated with the critical value, $(S/\omega)_i \approx (S/\omega)_{cr} = 0.135$.

For vortex pairs in background shear ($\zeta_0 \neq 0$), these properties are presented in figures S2 and S3 (A_{II} and Γ_{II} are normalized by their initial values); these figures correspond to the vortex-dominated cases shown in figures 3 and 4 in the main text. Figure S2c shows an example of no-shear merger, in which one can observe the behaviors just discussed. In the $\zeta_0 \neq 0$ cases, as discussed in the main text (§5.1), the time evolution of these quantities follows a similar pattern

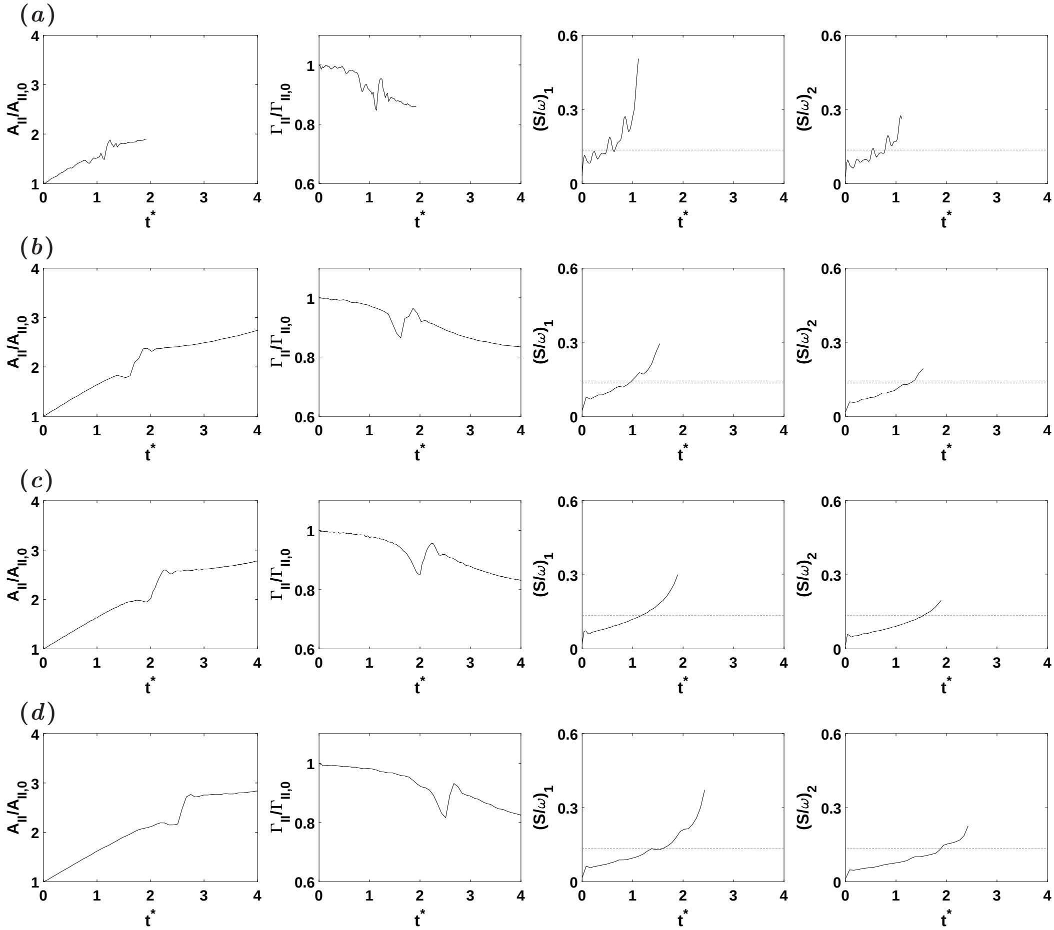

Figure S2: Time development of key quantities (aggregate normalized core area $A_{II}/A_{II,0}$ and circulation $\Gamma_{II}/\Gamma_{II,0}$, and relative straining of each vortex $(S/\omega)_i$, $i = 1, 2$) for the vortex-dominated cases shown in figure 3 of the main text, UPEA pairs having $Re_\Gamma = 5000$ and $\Lambda_0 = 0.90$, with varying shear strength ζ_0: (a) $\zeta_0 = 0.0167$, (b) $\zeta_0 = 0.0045$, (c) $\zeta_0 = 0$ (no shear), and (d) $\zeta_0 = -0.0045$. Dashed line in $(S/\omega)_i$ plots indicates critical relative straining $(S/\omega)_{cr} = 0.135$. The data in case (c) was previously presented in Folz & Nomura 2017.

to the no-shear case, with the primary exception of nonlinear troughs in the development of A_{II} and Γ_{II}, which correspond to times of amplified deformation of the vorticies due to the shear and concomitant local maxima, i.e. bumps, in the time development of $(S/\omega)_i$.

For a given Λ_0 (figure S2), as $|\zeta_0|$ increases, $(S/\omega)_i$ generally grows more rapidly and the bumps become larger. Also, smaller "secondary" bumps become apparent at high ζ_0, between those already discussed, i.e. at an orientation of the peak-peak axis approximately orthogonal to theirs (e.g. in figure 7a of the main text at $t^* \approx 0.4$). For a given ζ_0 (figure S3), when the pair is asymmetric the increase of $(S/\omega)_1$ is more rapid, and the bumps larger, than for $(S/\omega)_2$, with this disparity increasing with decreasing Λ_0 (indicating more disparate deformation amplification, seen in figures 3-4 of the main text). For highly disparate pairs

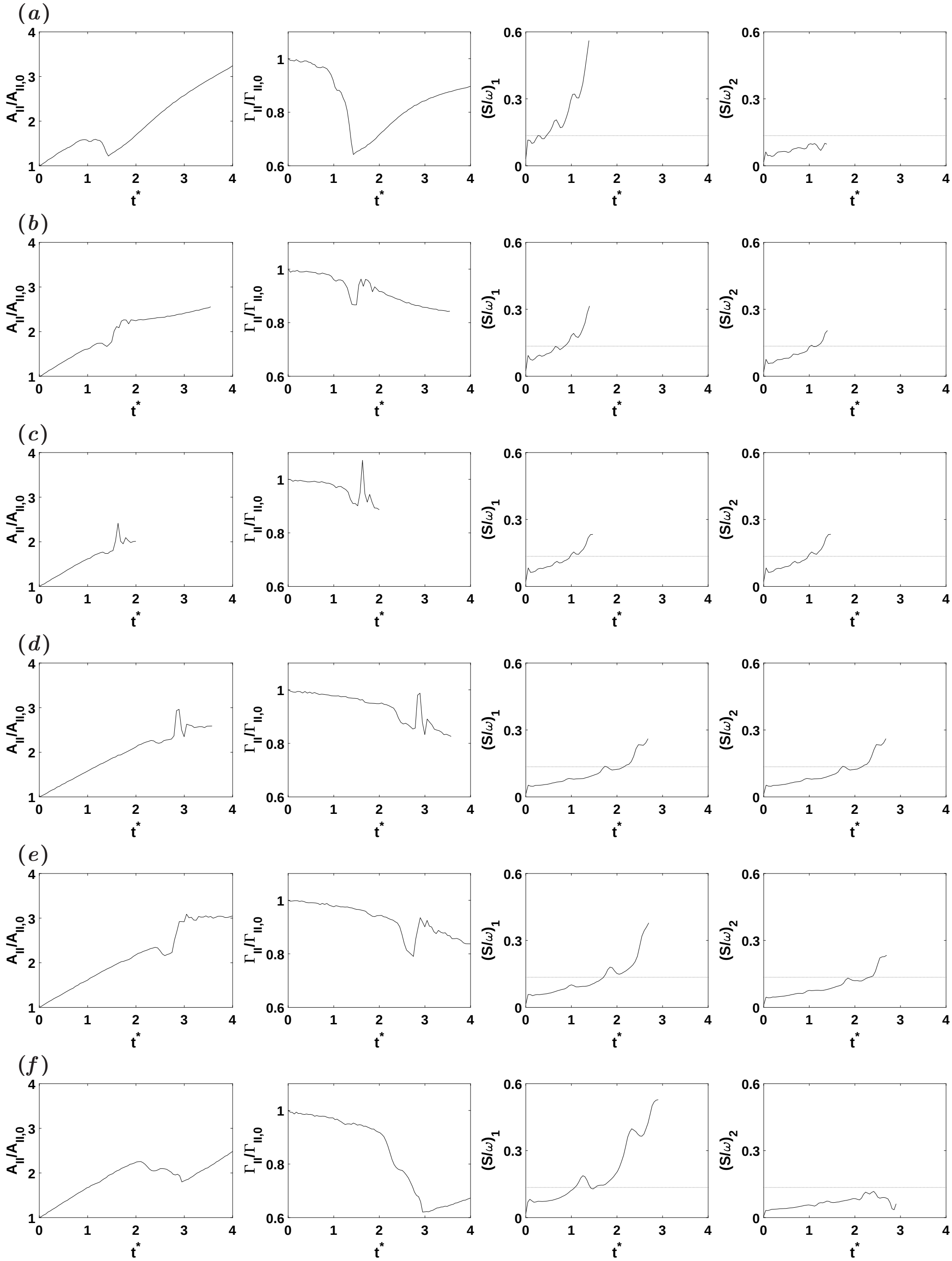

Figure S3: Time development of key quantities (aggregate normalized core area $A_{II}/A_{II,0}$ and circulation $\mathit{\Gamma}_{II}/\mathit{\Gamma}_{II,0}$, and relative straining of each vortex $(S/\omega)_i$, $i = 1, 2$) for the vortex-dominated cases shown in figure 4 of the main text, UPEA pairs having $Re_{\mathit{\Gamma}} = 5000$ and $|\zeta_0 = 0.0073|$, with varying $\mathit{\Lambda}_0$: (a) $\mathit{\Lambda}_0 = 0.7$, (b) $\mathit{\Lambda}_0 = 0.90$, (c) $\mathit{\Lambda}_0 = 1.0$ having favourable shear ($\zeta_0 = 0.0073$); (d) $\mathit{\Lambda}_0 = 1.0$, (e) $\mathit{\Lambda}_0 = 0.90$, and (f) $\mathit{\Lambda}_0 = 0.70$ having adverse shear ($\zeta_0 = -0.0073$). Dashed line in $(S/\omega)_i$ plots indicates critical relative straining $(S/\omega)_{cr} = 0.135$.

(typically $\Lambda_0 < 0.80$), the "bumps" in $(S/\omega)_2$ are low-amplitude and often multi-peaked, indicating minimal deformation amplification.

In all cases, the start of the significant slowing of A_{II} growth and acceleration of Γ_{II} decline — behaviors associated with the start of core detrainment in no-shear pairs — coincides with $(S/\omega)_1$ surpassing *and maintaining* $(S/\omega)_{cr} = 0.135$, the value associated with the onset of core detrainment of a vortex in a no-shear pair or in adverse background shear. It is also seen that, in the cases identified as mergers in figures 3 and 4 in the main text, $(S/\omega)_2$ also surpasses (S/ω_{cr}) at or after the time that $(S/\omega)_1$ does. Because of this, and the correspondence to qualitative observations of the vorticity contours, and the fact that these flows are vortex-dominated, these behaviors are taken to correspond to detrainment (and the spikes, entrainment) in these $\zeta_0 \neq 0$ pairs. The outcomes of these interactions and their quantitative assessment are discussed in §5.